Journal of the Marine Biological Association of the United Kingdom, 2013, 93(4), 855–866.
doi:10.1017/S0025315412000677

Spatial structuring of submerged aquatic vegetation in an estuarine habitat of the Gulf of Mexico

ARETHA MORIANA BURGOS-LEÓN[1], DAVID VALDÉS[1], MA. EUGENIA VEGA[1] AND OMAR DEFEO[2]

[1]Centro de Investigación y de Estudios Avanzados, Unidad Mérida, AP 73 Cordemex, 97310 Mérida, Yucatán, México,
[2]UNDECIMAR, Facultad de Ciencias, Iguá 4225, Montevideo, Uruguay

Seasonal changes in spatial structure of biomass of submerged aquatic vegetation (SAV) and environmental variables were evaluated in Celestun Lagoon, an estuarine habitat in Mexico. Geostatistical techniques were used to evaluate spatial autocorrelation and to predict the spatial distribution by kriging. The relative contribution of 11 environmental variables in explaining the spatial structure of biomass of SAV was evaluated by canonical correspondence analysis. Spatial partitioning between species of SAV was evident: the seagrasses Halodule wrightii *and* Ruppia maritima *dominated the seaward and central zones of the lagoon, respectively, whereas the green alga* Chara fibrosa *was constrained to the inner zone. The spatial structure and seasonal variability of SAV biomass were best explained by organic carbon in the sediments, salinity and total suspended solids in the water column. Analysis at different spatial scales allowed identifying the importance of spatial structure in biotic and abiotic variables of this estuarine habitat.*

Keywords: coastal lagoon, estuarine habitat, nutrients, seagrasses, alga, sediments, spatial structure, geostatistics, seasonal variability, México

Submitted 15 March 2012; accepted 22 April 2012; first published online 14 June 2012

INTRODUCTION

Submerged aquatic vegetation (SAV), particularly seagrasses and macroalgae, constitute a critical component of highly productive marine coastal ecosystems with complex physical structure. SAV provides a combination of food and shelter that enable a higher species richness than adjacent ecosystems (Travers & Potter, 2002; Ribeiro *et al.*, 2006) and high biomass and productivity levels of invertebrates and fishes (Raposa & Oviatt, 2000; Pérez-Castañeda & Defeo, 2004). SAV also provides an important nursery area for many species that support inshore and offshore fisheries (Short *et al.*, 2007; Arceo-Carranza *et al.*, 2010). This ecosystem plays a critical role in accumulation and stabilization of sediments (Larkum *et al.*, 2006; Short *et al.*, 2007), as well as in cycling coastal nutrients, accelerating nitrogen fixation and increasing diffusive nutrient flux to local waters (Short & McRoy, 1984). Loss of SAV habitats alters the flow of organic matter, nutrient cycles and food webs throughout coastal ecosystems where SAV exports organic matter (Bach *et al.*, 1986; Preen *et al.*, 1995), eventually leading to collapse of fisheries, degradation of water quality and the decline of other living resources (Kenworthy *et al.*, 2006; Orth *et al.*, 2006). Environmental variables (e.g. light, nutrients, salinity and sediment texture) mainly regulate the spatial variability of SAV spatial patterns (Istvánovics *et al.*, 2008), whereas freshwater discharges are also important in explaining temporal variations (Cyrus & Blaber, 1987).

Corresponding author:
O. Defeo
Email: odefeo@fcien.edu.uy

Celestun Lagoon (Mexico) is a tropical estuarine habitat of ~22.5 km long, in the Gulf of Mexico (Figure 1). The substratum of this microtidal shallow lagoon with an almost flat bottom is dominated by SAV beds, mainly composed of the green alga *Chara fibrosa* (C. Agardh ex Bruzelius) in areas with low salinity (<15), the seagrass *Ruppia maritima* (Linnaeus) in brackish waters (10–25 m) and the seagrass *Halodule wrightii* (Aschers) in areas with marine conditions (Chávez *et al.*, 1993; Pérez-Castañeda & Defeo, 2004; Herrera-Silveira, 2006). The lagoon has strong spatial gradients in environmental variables with seasonal fluctuations (Pérez-Castañeda & Defeo, 2004). In the present study we assessed spatio-temporal variations in SAV distribution and environmental variables (sediment and water), as well as the role played by these variables in explaining SAV distribution in Celestun Lagoon.

MATERIALS AND METHODS

Study area

Celestun Lagoon is located in the north-west of the Yucatan Peninsula (20°45′N 90°25′W) in the Gulf of Mexico. It has an area of 28.14 km² and is connected to the sea by a 0.46 km wide mouth (Figure 1). It is a microtidal shallow lagoon with flat bottom, a mean depth of 1.2 m and a narrow tidal channel with a maximum depth of 3 m (Pérez-Castañeda & Defeo, 2004). Celestun Lagoon is characterized by high and constant turbidity because of continuous sediment resuspension and diffusion of 'tannins' from mangroves throughout the lagoon (Pérez-Castañeda & Defeo, 2004). As there are no

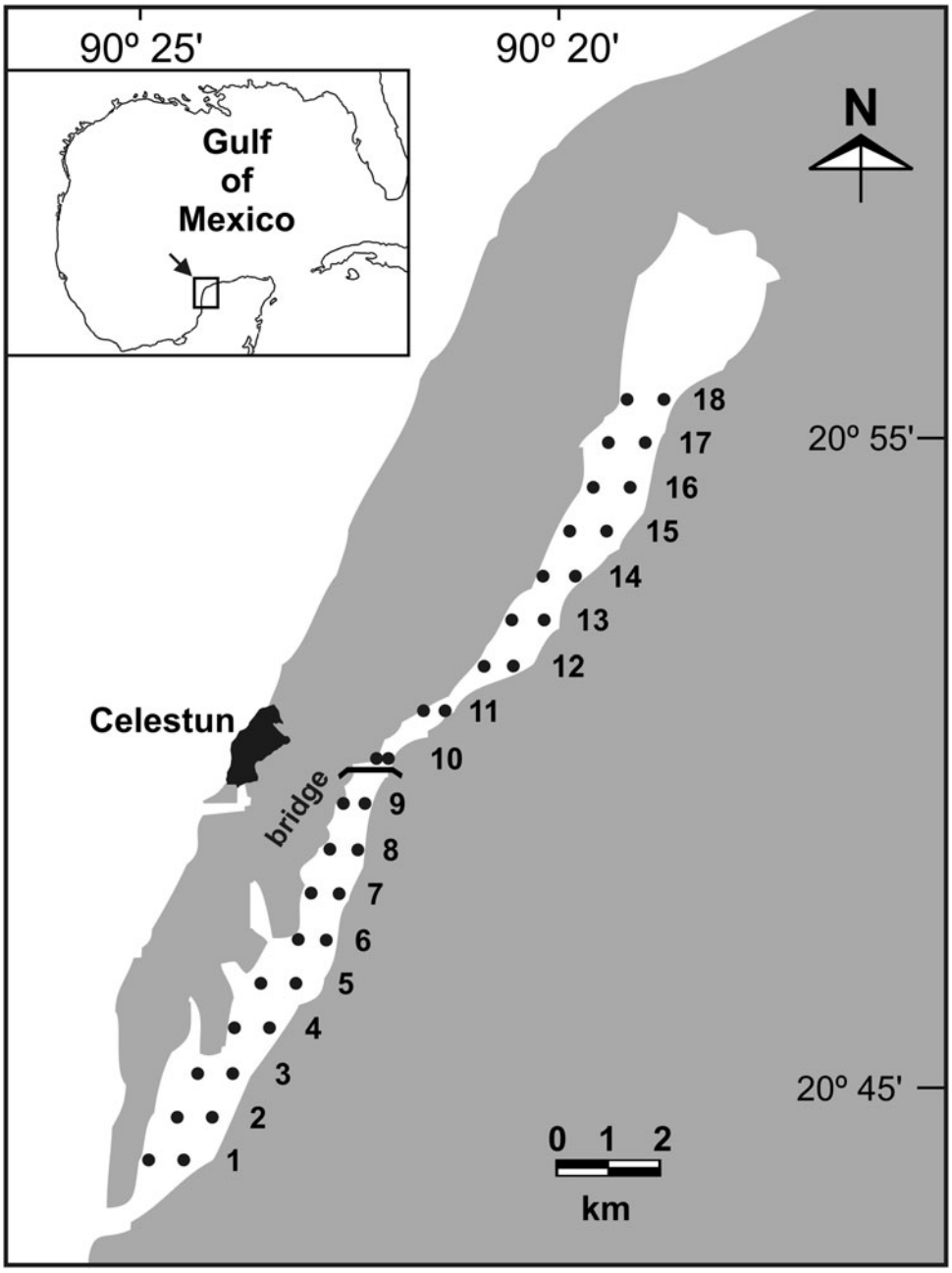

Fig. 1. Location of sampling sites (•) along the estuarine habitat of Celestun Lagoon, Mexico. 1–18: distance (km) from the mouth of the lagoon.

rivers, the spatial salinity gradient is conditioned by groundwater discharges (via freshwater springs in the northern part of the lagoon), tides and climatic seasons (Dry, March to May; Rainy, June to October; and Nortes (fronts), November to February). The Dry season is characterized by little rainfall (0–50 mm month^{-1}) in comparison to the Rainy season (>500 mm month^{-1}). Whereas the Dry and Rainy seasons are characterized by south-west winds <15 km h^{-1}, the Nortes season is affected by strong winds from the north (80 km h^{-1}), little rainfall (20–60 mm month^{-1}) and cool air temperatures (22°C) (Herrera-Silveira, 1994).

Sampling and laboratory procedures

We conducted three seasonal sampling surveys during February, April and September 2005, corresponding to the 'Nortes', 'Dry' and 'Rainy' seasons, respectively. We selected 18 pairs of sites from the outer to the inner zone of the lagoon at 1 to 1.5 m depth. Distance between consecutive pair of sites was 1 km (Figure 1). All samplings were carried out under the same conditions (depth and time of day) in order to minimize the effects on sample efficiency associated with sampling conditions. In order to complete each survey during one morning, three teams sampled the lagoon simultaneously.

Four sediment samples were taken in each site with a hand corer (5 cm diameter) to estimate grain size, organic carbon (OC), total nitrogen (TN) and total phosphorus (TP). OC was determined following the methods of Buchanan (1984), whereas TN and TP were obtained by wet oxidation of the dried sediments with potassium persulphate in basic and acidic conditions, respectively (Parsons *et al.*, 1984; Adams,

https://doi.org/10.1017/S0025315412000677 Published online by Cambridge University Press

1990). Grain size was estimated by suspending the sediment and measuring the density with a hydrometer.

Water samples were taken with Van Dorn bottles, stored at 4°C and brought into the laboratory for further analyses. pH was taken with a Beckman Phi-32 pH meter and combined glass electrode (NBS scale). In the laboratory, total suspended solids (TSS) were determined following the methods of Stirling (1985). The salinity of the filtered water was recorded using a salinometer (Kahlsico RS-9). Ammonium, nitrites, nitrates, phosphates and silicates were quantified using colorimetric techniques (Strickland & Parsons, 1972; Parsons *et al.*, 1984) with a Shimadzu 1201 UV/VIS spectrophotometer.

At each site, three replicate SAV samples (0.2 m^2 each) were taken, bagged and placed on ice for later analyses. In the laboratory, the SAV was rinsed free of sediment, sorted to species level (Littler & Littler, 2000) and oven-dried for 24 hours to a constant weight at 60°C to determine biomass (dry weight, g m^{-2}). Rhizomes (horizontal stem found underground) were considered for biomass estimations.

Spatial structure: geostatistics

A geostatistical appraisal was performed to examine the spatial structure and distribution of sedimentological and water variables, and SAV biomass (total and specific) along the estuarine–lagoon habitat. Geostatistics focus on the detection, modelling, and estimation of spatial patterns in spatially correlated data (Rossi *et al.*, 1992). Spatial autocorrelation occurs when samples collected close to each other are often more similar than samples collected farther apart, particularly when the variable sampled is spatially structured (e.g. in patches). Geostatistics usually involve 2 steps (Robertson, 1987): (1) characterizing the spatial structure of the variable by means of a variogram, thus defining the degree of autocorrelation among the data points; and (2) predicting values between measured points based on the estimated degree of autocorrelation. The spatial structure of a dataset is usually described by an empirical variogram, which is basically a plot of the variance or difference between pairs of observations against their distance in geographical space (Wagner, 2003). Variogram parameters are used for interpolating values, using a kriging algorithm that provides an error term for each value estimated, giving a measure of reliability for the interpolations (Robertson, 1987, 2000). In this paper, variographic analysis and punctual kriging were used to characterize the SAV spatial structure and make local predictions. In accordance with the main objective of this study, a one dimensional approach was used. The spatial autocorrelation of these variables was evaluated by semivariance analysis through variograms, which quantify the spatial dependence between them. Changes in semivariance within a variogram represent the rate of deterioration of the influence of a given sample over increasingly remote zones in the study area (Matheron, 1963). To this end, mean values of SAV biomass (total and specific) and sedimentological and water variables were calculated for each pair of sampling sites along the coastal lagoon. The 1-dimensional transects consisted of 18 mean observations measured at a location x defined with respect to its relative distance from the mouth of Celestun Lagoon (1 to 18 km) (Pérez-Castañeda & Defeo, 2004). Because variograms tend to decompose at large lag intervals close to the maximum lag interval, the active lag distance used in the variographic analysis was close to 80% of the maximum lag.

A variogram $\gamma(h)$ was estimated for each one dimensional transect (consisting of 18 mean values of the variable studied) using Matheron's (1965) estimator:

$$\gamma(h) = \frac{\sum_{i=1}^{Nh} [Z(x_i + h) - Z(x_i)]^2}{2N(h)}$$

where $Z(x_i)$ is the measured sample value at location x_i, $Z(x_i + h)$ is another measured sample value separated from x_i by a distance h (measured in km), and $N(h)$ is the number of pairs of observations separated by h. Several theoretical models (spherical, exponential, Gaussian and linear) were fitted to the experimental variograms. The models provide the following parameters (Robertson, 1987): (1) the nugget-effect (C_o), which reflects the spatial variability below the minimum lag distance that cannot be modelled with the current sampling resolution (i.e. 1 km in this case); (2) the sill ($C_o + C$), which defines the asymptotic value of semivariance; and (3) the range (A_o), defined as the distance over which autocorrelation is present (Cressie, 1991). These parameters allow the proportion of sample variance explained by the spatially structured component $C/(C_o + C)$ to be estimated. A variable is spatially structured if the proportion of sample variance ($C_o + C$) that is explained by spatially structured variance C tends to 1. In this case, the variogram with no nugget variance and the curve passes through the origin. The different variograms were defined as:

Spherical:

$$\gamma(h) = C_o + C\left[1.5\left(h/A_o\right) - 0.5\left(h/A_0\right)^3\right] \quad \text{for } h \le A_o$$
$$\gamma(h) = C_o + C \quad \text{for } h > A_o$$

Gaussian:

$$\gamma(h) = C_o + C[1 - \exp(-h^2/A_o^2)]$$

Here, the effective range is given by $A = 3^{0.5}\, A_o$, which is the distance at which the sill ($C + C_o$) is within 5% of the asymptote.

Exponential:

$$\gamma(h) = C_o + C[1 - \exp(-h/A_o)]$$

With the effective range being $A = 3A_o$, which is the distance at which the sill ($C + C_o$) is within 5% of the asymptote. The sill never meets the asymptote in the exponential or Gaussian models.

The model fitting procedure used the reduced sum-of-squares of the residuals (RSS) to choose parameters for each of the variogram models by determining a combination of parameter values that minimizes RSS for any given model (see details in Robertson, 2000). The coefficient of determination (r^2) was also used as an additional indicator of goodness of fit, even though this estimate is not as robust as the RSS for best-fit calculations.

Once spatial dependence had been determined, variogram parameters to interpolate values along each transect for points not measured through punctual kriging (Matheron, 1965) were used. Punctual kriging provides an error term for each

https://doi.org/10.1017/S0025315412000677 Published online by Cambridge University Press

estimated value, therefore giving a measure of reliability for the interpolations. Subsequently, kriging values were used to validate the fitted variogram through cross-validation. This procedure is based on the systematic removal of observations from the raw data set, one by one, which were then estimated by kriging. Estimated (E) versus observed (O) values were fitted to a linear regression of the form $O = \alpha + \beta E$, and departures from a 1-to-1 line through the origin indicated model inadequacy. The simultaneous F test (Dent & Blackie, 1979) was used to test the null hypothesis of slope = 1 and intercept = 0. After modelling the spatial autocorrelation and validating the fitted variogram, a transect image of the analysed variable, including observed data, interpolations, and the variance of interpolations, was generated. Interpolation was not carried out in cases where spatial autocorrelation was not detected and only the observed data were plotted to depict any spatial trend. An analysis of covariance (ANCOVA) was performed for salinity and silicates, with season as the main factor, distance as the covariate, and log (salinity or silicates) as the dependent variable. This analysis was restricted to km 2 to 18 in order to fulfil ANCOVA requirements.

Relationship between SAV distribution and environmental variables

Multivariate analysis was used to assess the relative effect of sedimentological and water variables on SAV distribution and biomass. Canonical correspondence analysis (CCA) was chosen for modelling, since gradient length and eigenvalues suggested a unimodal model (Dodkins *et al.*, 2005). Variance inflation factors (VIFs) were assessed: a high value for the VIF (>20) indicates multicollinearity between variables (Ter Braak, 1986) and thus the variable with the highest VIF was removed. This procedure was repeated until all VIF values were <10. Statistical tests were carried out using a Monte Carlo simulation with 499 permutations (Ter Braak & Smilauer, 2002). The analysis was performed using the computer program CANOCO 4.5 (Ter Braak & Smilauer, 2002).

RESULTS

Spatial analysis

SEDIMENTS

Organic carbon was always spatially structured (Table 1). In Nortes and Rainy seasons the spatial structure was best characterized by a spherical variogram, and in the Dry season by a Gaussian variogram (Figure 2; Table 1). OC variograms revealed a high and stable spatial structure ($C/(C_o + C)$ >94%). The distance of spatial influence, A_o (interpreted as patch size), was 10.26 km, 10.48 km and 3.55 km in the Nortes, Dry and Rainy seasons, respectively (Table 1). In the three climatic seasons OC tended to show higher concentrations between sites 3 and 6, decreasing towards the inner zone of the lagoon. The Dry season presented the lowest OC concentrations (Figure 3).

Total phosphorous concentrations only presented a marked spatial structure during the Dry season, and were best modelled by a spherical variogram, which presented a high and stable spatial structure and a spatial autocorrelation distance of 8.41 km (Table 1; Figure 2). The transect image presented the highest concentrations at site 2, gradually decreasing to their lowest between sites 7 and 12, increasing again between sites 13 and 16 (Figure 3).

Total nitrogen structure was best represented by a spherical variogram during Nortes, with a high and stable spatial structure and a spatial autocorrelation distance A_o of 4.56 km (Table 1; Figure 2). The transect image displayed the highest concentrations between sites 3 and 6 (Figure 3). No structuring was displayed in Rainy and Dry climatic seasons.

Sediment grain size did not display spatial structure, but decreased linearly from the mouth of the lagoon towards the inner zone. The ANCOVA performed with climatic season as main factor, distance (D) (2 to 18 km) as the covariate and grain size as the dependent variable, showed that for the same D, grain size significantly varied between seasons ($F_{2,48} = 8.90$; $P < 0.01$), with the lowest values in the Rainy season (Tukey test: $P < 0.001$).

WATER

Silicates, salinity and pH showed clear spatial gradients along the lagoon, and a lack of spatially organized internal structure (Figure 4). Silicate concentration decreased from the inner zone seawards because of an influx of groundwater in the inner zone of the lagoon (Figure 4A). This continuous spatial gradient of silicates (Si) followed an exponential function of the form: $Si = ae^{(bD)}$ where a and b are significant parameters ($P < 0.01$). Silicates varied between seasons (ANCOVA: $F_{2,48} = 107.06$), being significantly higher in the Rainy season (207.28 to 395.88 μM) than in Nortes (61.65 to 305.98 μM) and Dry (18.18 to 214.90 μM) seasons (Tukey test, $P < 0.0001$).

Salinity (S) decreased from the seaward end (site 1) to the innermost zone (site 18) of the lagoon, following a monotonically decreasing exponential function of distance (D) from the mouth of the lagoon of the form: $S = ae^{(-bD)}$, where a and b are significant parameters (Figure 4B). Salinity significantly differed between seasons (ANCOVA: $F_{2,\ 50} = 164.13$), with the highest values in the Dry season (28.02 to 37.40) and the lowest ones in the Rainy season (8.33 to 22.43) (Tukey test, $P < 0.001$).

The pH linearly increased with distance (D) from the mouth of the lagoon (Figure 4C), following the model $pH = a + bD$, where a and b are significant parameters ($P < 0.01$). The pH significantly differed between climatic seasons (ANCOVA: $P < 0.01$), being higher in the Rainy season than in Nortes and Dry seasons (Tukey test, $P < 0.0001$).

Ammonium was spatially-structured in the Nortes and Rainy seasons (Table 1). The structure was best characterized by spherical variograms with a stable spatial structure $C/(C_o + C) \geq 99\%$. The spatial influence distance, A_o was 2.86 and 2.62 km in the Nortes and Rainy seasons respectively (Table 1; Figure 2), where ammonium concentrations were highest at sites 17 and 18 (Figure 3).

Nitrates were highly spatially structured (>95%) in all three climatic seasons (Table 1), and best characterized by spherical (Nortes and Dry seasons) and Gaussian (Rainy season) variograms (Figure 2). A_o was 9.58 km for the Nortes season, 9.52 km for the Dry season and 7.83 km for the Rainy season (Table 1; Figure 2). The transect image showed the highest concentrations between sites 6 and 15, particularly during the Rainy season (Figure 3).

https://doi.org/10.1017/S0025315412000677 Published online by Cambridge University Press

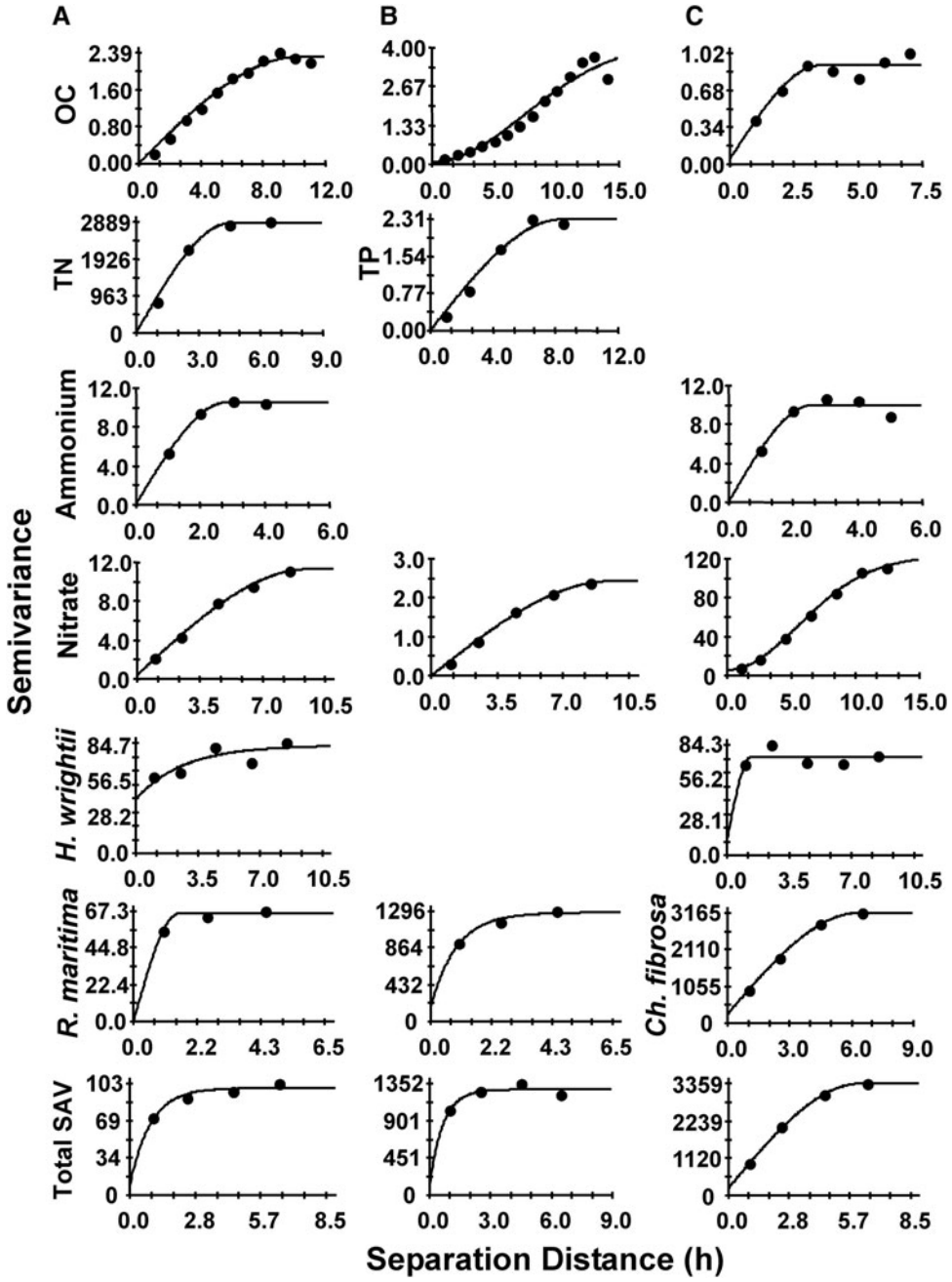

Fig. 2. Theoretical variograms fitted for sediment and water variables, and submerged aquatic vegetation biomass in: (A) Nortes, (B) Dry and (C) Rainy seasons. Details of variogram models are shown in Table 1. Mean values of each variable along the one dimensional transect were used. Note the different scales of X and Y axes. Spatial autocorrelation was not detected in some cases (not shown).

SUBMERGED AQUATIC VEGETATION (SAV)

Halodule wrightii was spatially structured in Nortes and Rainy seasons and best characterized, respectively, by exponential and spherical variograms (Table 1). Variograms showed that spatially structured component $C/(C_o + C)$ was always $\geq$50%. The spatial influence distance (A_o) was 2.68 km (Nortes) and 1.36 km (Rainy) (Table 1; Figure 2). In Nortes, *Halodule wrightii* presented a continuous distribution with no definite alongshore pattern, being absent from km 15 to inner waters (Figure 3). In the Rainy season, *H. wrightii* showed a continuous distribution along the lagoon, with the highest biomass at sites 3, 4, 10 and 14. *Ruppia maritima* presented spatial structuring in Nortes and Dry seasons, being modelled, respectively, by spherical and exponential variograms [$C/(C_o + C) > 85\%$]. The spatial influence distance A_o was 1.54 km in Nortes and 2.76 km in the Dry season (Table 1; Figure 2). In Nortes, *R. maritima* biomass was highest between km 12–13 and 15–16, while in the Dry season peaked between sites 11 and 16, with a biomass four times greater than in Nortes (Figure 3). *Chara fibrosa* presented spatial structure in the Rainy season and was best represented by a spherical variogram [$C/(C_o + C) > 90\%$] and $A_o = 6.3$ km (Table 1), and its highest biomass was found between sites 13 and 17 (Figure 3). Total SAV was best represented in Nortes and Dry seasons by exponential variograms, and in the Rainy season by a spherical variogram

https://doi.org/10.1017/S0025315412000677 Published online by Cambridge University Press

Table 1. Parameters and goodness of fit criteria for variographic and cross-validation analyses of punctual kriging estimates for sediment and water variables (TP, total phosphorus; TN, total nitrogen) and submerged aquatic vegetation (SAV) species (*Halodule wrightii*, *Ruppia maritima*, *Chara fibrosa* and total vegetation) in N, Nortes, D, Dry, R, Rainy seasons, in Celestun Lagoon. Mean values of each variable along a one dimensional transect were used. Sphe (spherical), Gauss (Gaussian) and Exp (exponential); C_o, nugget effect; $C_o + C$, asymptotic semivariance; A_o, distance (km) over which autocorrelation occurs; % spatially structured component $[C/(C_o + C)]$; r^2 coefficient of determination; RSS, reduced sum of squares; Bias: simultaneous F statistic for slope = 1 and intercept = 0; in all cases $P > 0.05$. Only those cases with spatial structure are shown.

		Sediment					**Water**				
		Organic carbon (%)			**TP(μmol/g)**	**TN(μmol/g)**	**Ammonium(μmol/g)**		**Nitrates(μmol/g)**		
	Seasons	**N**	**D**	**R**	**D**	**N**	**N**	**R**	**N**	**D**	**R**
Theoretical variogram	Model	Sphe	Gauss	Sphe	Sphe	Sphe	Sphe	Sphe	Sphe	Sphe	Gauss
	C_o	0.00	0.08	0.04	0.00	1.00	0.09	0.01	0.39	0.00	5.80
	C_o+C	2.29	4.17	0.91	2.31	2853.0	10.56	9.99	11.29	2.42	122.3
	A_o	10.26	10.48	3.55	8.41	4.56	2.86	2.62	9.58	9.52	7.83
	%	100	98.1	94.9	100	100	99.1	99.9	96.5	100	95.3
	RSS	0.09	0.88	0.03	0.07	23123	0.04	2.05	0.19	0.02	26.4
	r^2	0.99	0.96	0.88	0.99	0.99	0.99	0.89	0.99	0.99	0.99
Cross-validation	a	−0.01	0.11	−0.06	−0.01	−32.26	1.89	1.61	0.33	−0.04	0.81
	b	0.98	0.95	1.02	0.99	1.14	0.88	0.91	0.95	1.01	0.93
	r^2	0.81	0.82	0.59	0.82	0.72	0.31	0.30	0.59	0.79	0.77
	Bias	0.27	3.31	0.29	0.02	0.03	1.13	0.79	0.27	0.22	0.08
			SAV								
			H. wrightii (gm^{-2})		*R. maritima* (gm^{-2})		*Ch. fibrosa* (gm^{-2})		Total vegetation (gm^{-2})		
	Seasons	N	R		N	D	R	N		D	R
Theoretical variogram	Model	Exp	Sphe		Sphe	Exp	Sphe	Exp		Exp	Sphe
	C_o	41.3	12.3		0.10	185	272	8.9		128	221
	C_o+C	82.61	75.34		65.76	1280	3165	98.7		1282	3350
	A_o	2.68	1.36		1.54	2.76	6.33	2.63		1.91	6.12
	%	50.0	83.7		99.8	85.5	91.4	91.0		90.0	93.4
	RSS	180	128		4.6	2189	679	37.4		9901	3881
	r^2	0.68	0.18		0.94	0.97	1.00	0.93		0.82	0.99
Cross-validation	a	3.56	29.86		−5.56	4.21	0.27	2.18		9.60	−1.08
	b	0.52	−3.83		2.05	0.71	0.94	0.80		0.50	0.97
	r^2	0.04	0.24		0.16	0.09	0.61	0.10		0.02	0.64
	Bias	0.04	2.38		0.08	0.00	2.24E-05	0.47		$4.8X10^{-3}$	1.02E-05

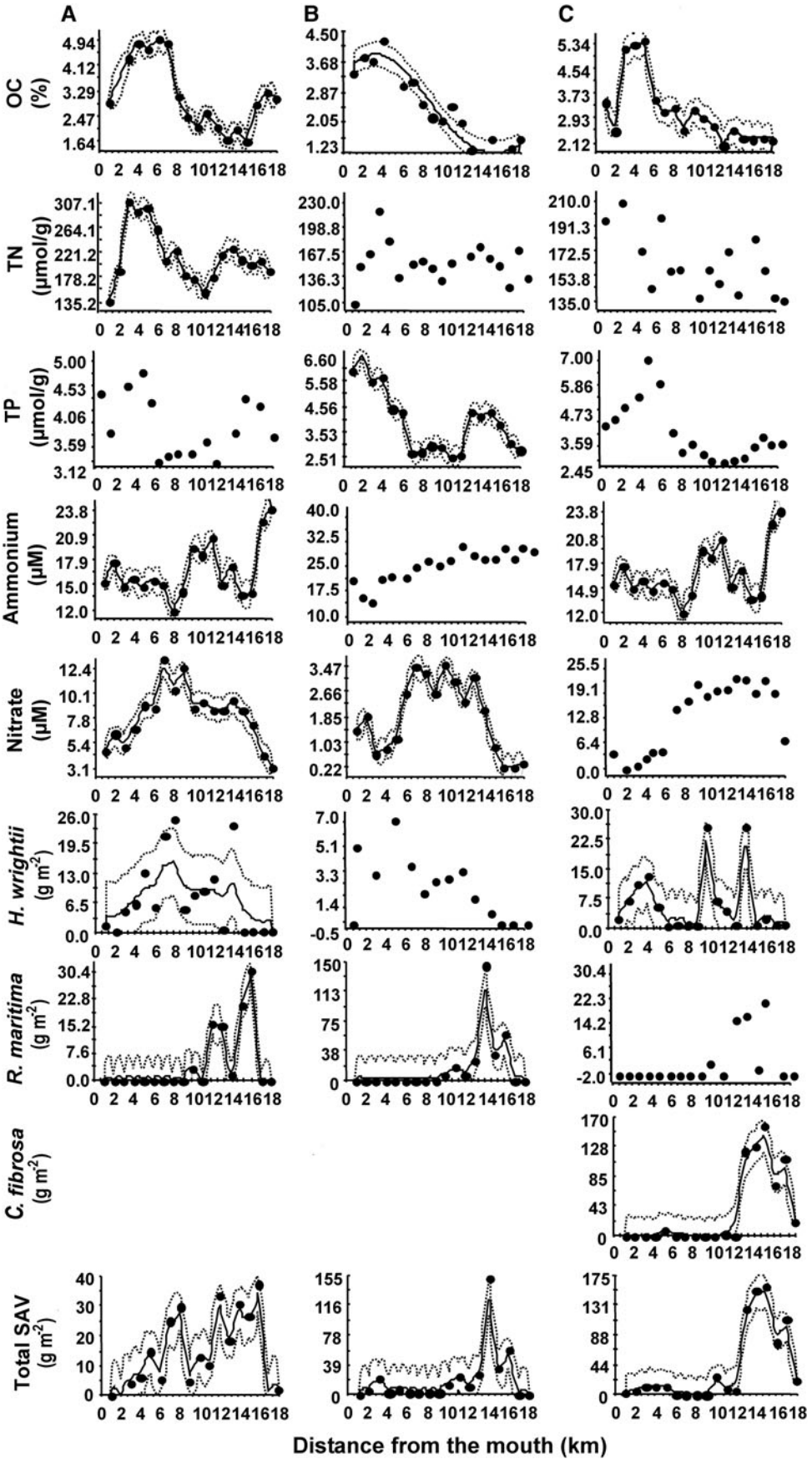

Fig. 3. Transect images for each season ((A) Nortes, (B) Dry and (C) Rainy) generated with punctual kriging, showing observed (•) and predicted mean (continuous lines) ± SD (dotted lines) biomass for environment variables in sediment water and seagrasses *Halodule wrightii* and *Ruppia maritima*, green alga *Chara fibrosa*, and total submerged aquatic vegetation along the estuarine habitat. Note different scales of Y-axes.

https://doi.org/10.1017/S0025315412000677 Published online by Cambridge University Press

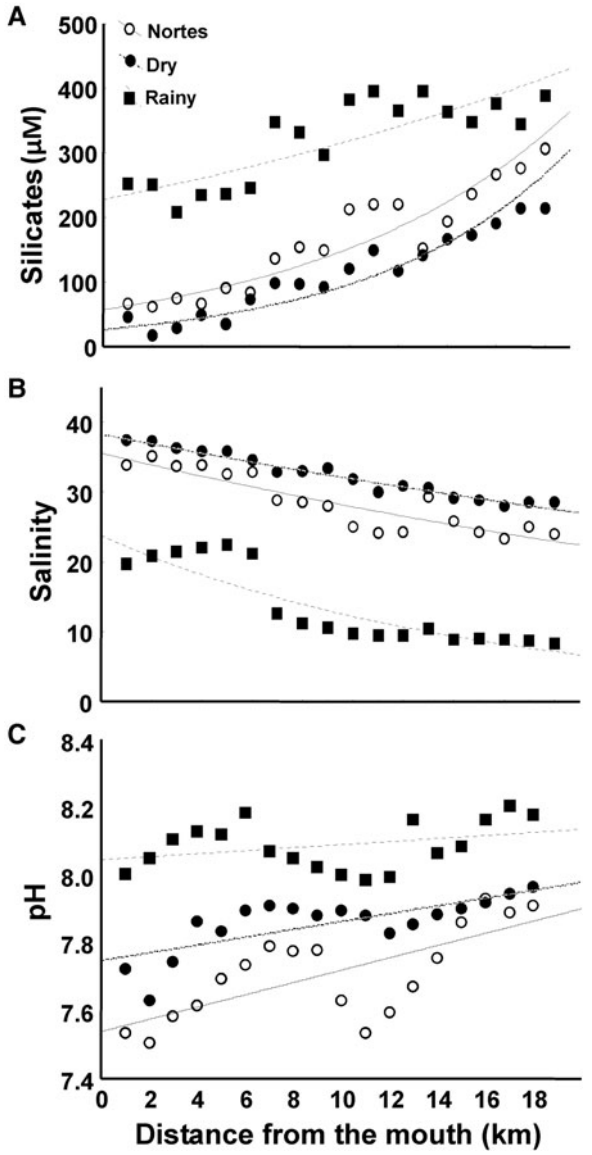

Fig. 4. Seasonal variations in silicates, salinity and pH along Celestun Lagoon. Data points correspond to mean values over 1 to 18 km. Exponential decay models fitted for each season are shown.

with a structure ≥90% and A_o values of 2.63 km in Nortes, 1.91 km in the Dry season and 6.12 km in the Rainy season (Table 1).

Relationship between environmental variables and SAV

SEDIMENT

The first CCA axis explained most of the variance in sediment variables (OC, TP, TN and grain size) as follows (Table 2): Nortes 49%, Dry 53% and Rainy 45%. Significant eigenvalues were 0.539 in the Dry season and 0.455 in the Rainy season. The variance explained (marginal effects) by TP, TN and grain size was small (≤13.87%) in the three seasons (Table 3). OC was significant in the Dry and Rainy seasons (conditioned effect: $P < 0.05$), and best structured the SAV biomass: the variance explained in the Dry season was 24.09% and in the Rainy season was 36.26% (Table 4).

Table 2. Canonical correspondence analysis of sediment and water variables in Celestun Lagoon for submerged aquatic vegetation species. Eigenvalues of the first two axes, variance explained, and *F* and *P* values for the first axis are detailed for each climatic season.

	Axes				
	Eigenvalue		Variance explained		
Sediment	**1**	**2**	**(%)**	***F***	***P***
Nortes	0.474	0.016	49	1.624	0.176
Dry	0.539	0.125	53	10.742	0.004
Rainy	0.445	0.012	45	6.135	0.006
Water					
Nortes	0.565	0.353	91	3.047	0.004
Dry	0.637	0.028	63	30.83	0.002
Rainy	0.537	0.018	55	7.133	0.002

In Nortes, the ordination diagram for sediment variables showed that grain size was the most important explanatory variable of SAV variation. Abundance of *H. wrightti* was negatively associated with grain size, *R. maritima* with OC, and *Ch. fibrosa* with TN and TP (Figure 5A). For the Dry season, SAV variation was mostly related to OC. *Ruppia maritima* exhibited a positive association with grain size, and a negative association with OC, TP and TN (Figure 5B). For the Rainy season (Figure 5C), OC best explained variations in SAV. SAV biomass at sites 15–18 followed a clear association with *Ch. fibrosa*, which in turn was negatively associated with OC, TN and TP. The distribution at sites 6–13 showed association with *R. maritima.*

WATER

The first axis of the CCA explained 91% of the variance in Nortes, 64% in Dry and 54% in Rainy seasons. The relationships between response and explanatory variables were significant for the three climatic seasons (Monte Carlo test: $P < 0.05$), with eigenvalues of 0.56, 0.64 and 0.54 respectively (Table 2). Nitrites (all seasons), silicates (Nortes and Dry seasons) and salinity (Rainy season) were omitted because collinearity > 10. Individually, nitrates, phosphates, silicates and TSS variables in the three seasons explained <9%.

Table 3. Canonical correspondence analysis variance partitioning analysis explained by each variable (sediment and water) individually (marginal effects) in three climatic seasons in Celestun Lagoon.

Environmental variable	**Variance (%)**		
Sediment	**Nortes**	**Dry**	**Rainy**
Organic carbon	10.13	24.09	36.96
Total phosphorus	6.39	0.15	6.30
Total nitrogen	2.24	0.45	0.42
Grain size	13.87	0.00	3.86
Water			
Ammonium	22.43	0.00	0.57
Nitrates	7.21	0.45	0.03
Phosphates	5.64	0.60	5.44
Silicates	–	–	0.57
pH	14.00	3.46	1.14
Salinity	6.66	26.66	–
Total suspended solids	1.90	2.86	8.74

–, absent values because of colinearity.

https://doi.org/10.1017/S0025315412000677 Published online by Cambridge University Press

Table 4. Environmental variables (marginal effects = λ_1) in canonical correspondence analysis for sediment and water variables of three estuarine-lagoon species of submerged aquatic variation in Celestun Lagoon, in N, Nortes, D, Dry and R, Rainy seasons. Total inertia = 1.47. * $P < 0.05$. R**, silicates against salinity because of colinearity. Abbreviations of variables are detailed in Figure 5.

	OC			TP			TN			Grain size		
Season	**N**	**D**	**R**	**N**	**D**	**R**	**N**	**D**	**R**	**N**	**D**	**R**
Mean	3.31	2.50	3.14	3.95	3.98	3.97	213.58	159.98	166.72	2.42	2.70	2.11
Minimum	1.07	0.07	1.09	1.68	1.72	1.88	36.84	88.72	75.73	1.08	0.94	0.65
Maximum	10.01	6.46	8.24	5.27	8.38	11.19	406.57	243.57	271.02	3.13	3.76	2.88
Units	%	%	%	µmol/g	µmol/g	µmol/g	µmol/g	µmol/g	µmol/g	Φ	Φ	Φ
λ_1	0.14	0.16*	0.25*	0.09	0.001	0.044	0.033	0.003	0.003	0.20	0.00	0.02

	Ammonium			Nitrate			Phosphate			pH			Salinity Si			TSS		
Season	**N**	**D**	**R**	**N**	**D**	**R**	**N**	**D**	**R**	**N**	**D**	**R**	**N**	**D**	**R****	**N**	**D**	**R**
Mean	16.5	23.4	13.3	8.0	1.8	3.9	1.2	0.3	41.6	7.7	7.8	8.0	28.5	32.4	320.0	40.0	49.7	20.9
Minimum	7.0	9.8	1.98	3.1	0.2	2.3	0.0	0.1	7.0	7.3	7.5	7.9	20.7	26.3	171.2	9.56	16.4	2.0
Maximum	31.1	33.9	69.9	13.2	3.5	22.1	0.8	0.5	68.9	7.9	8.0	8.3	35.3	37.7	432.0	154.2	127.6	107.6
Units	µM	µM	µM	µM	µM	µM	µM	µM	µM	–	–	–	‰	‰	µM	mg/l	mg/l	mg/l
λ_1	0.33	0.00	0.00	0.11	0.00	0.02	0.08	0.00	0.03	0.20	0.02*	0.00	0.09	0.17*	0.00	0.02	0.01*	0.06*

Ammonium (Nortes); pH, salinity and TSS (Dry season); and TSS (Rainy season) significantly (conditioned effect: $P < 0.05$) explained spatial variations in SAV biomass (Table 3). CCA for Nortes showed that nitrates, phosphates and salinity best explained distributional patterns of SAV, whereas salinity and TSS were the most important variables for the Dry and Rainy seasons, respectively (Figure 5).

DISCUSSION

Geostatistical analysis revealed autocorrelation in SAV samples, and thus variographic analyses successfully explained the spatial structure of SAV. The biomass of *H. wrightii*, *R. maritima* and *Ch. fibrosa* displayed wide variations in spatial structure between climatic seasons, both in abundance and patch size (A_o) that in most cases varied in more than 100%. The green alga *Ch. fibrosa* presented a strong spatial structure in the Rainy season and almost disappeared in Nortes and Dry seasons (salinity >34), because it is mainly associated with low salinity conditions (Pérez-Castañeda & Defeo, 2004; Herrera-Silveira, 2006). By contrast, *R. maritima* was spatially structured and its biomass was particularly highest in the Dry season, taking advantage of high salinity levels (>30) (Pérez-Castañeda & Defeo, 2004; Herrera-Silveira, 2006), even though it can colonize marine, estuarine and freshwater habitats (Lazar & Dawes, 1991). Finally, *H. wrightii* was spatially structured in Nortes and Rainy seasons, with low biomass and intermittent occurrence from sites 1 to 14. Similar patterns of spatial structure have been detected in other seagrasses, also using geostatistical techniques (Zupo *et al.*, 2006). Variations in persistence of a spatial structure in plant communities through time could occur in the forms of (Wagner, 1993): (1) single-species aggregation and dispersion patterns; (2) distance-dependent interactions between species; and (3) the response to the spatial structure of environmental conditions. In this paper, spatio-temporal trends in abundance and patch size of the three SAV species could result from a combination of vegetative expansion and a differential response to the spatial structure of environmental conditions, notably salinity. In this context, experimental results showed that *R. maritima* has a competitive advantage over other seagrasses (e.g. *H. wrightii*) by having broader tolerances to salinity and temperature and an earlier annual growth cycle (Lazar & Dawes, 1991). Moreover, vegetation maps of the lower Laguna Madre prepared from long-term surveys showed a decrease in cover by *H. wrightii*, concurrently with an increase in other seagrass species, in deeper parts of the lagoon (Quammen & Onuf, 1993). Turbidity caused by maintenance dredging and reductions in salinity maxima were suggested by these authors as critical drivers that have limited expansion rates of seagrasses into suitable habitats. This is of utmost importance, given that hypo- and hyperosmotic conditions could inhibit photosynthesis in seagrasses (Touchette, 2007). Thus, the differential tolerance among species to salinity variations, which characterizes estuarine systems such as Celestun Lagoon, could explain spatio-temporal trends in SAV biomass.

Multivariate ordination techniques were also useful to describe multispecies SAV responses to environmental factors. The spatial distribution of the SAV biomass along the estuarine habitat was best explained by the salinity

https://doi.org/10.1017/S0025315412000677 Published online by Cambridge University Press

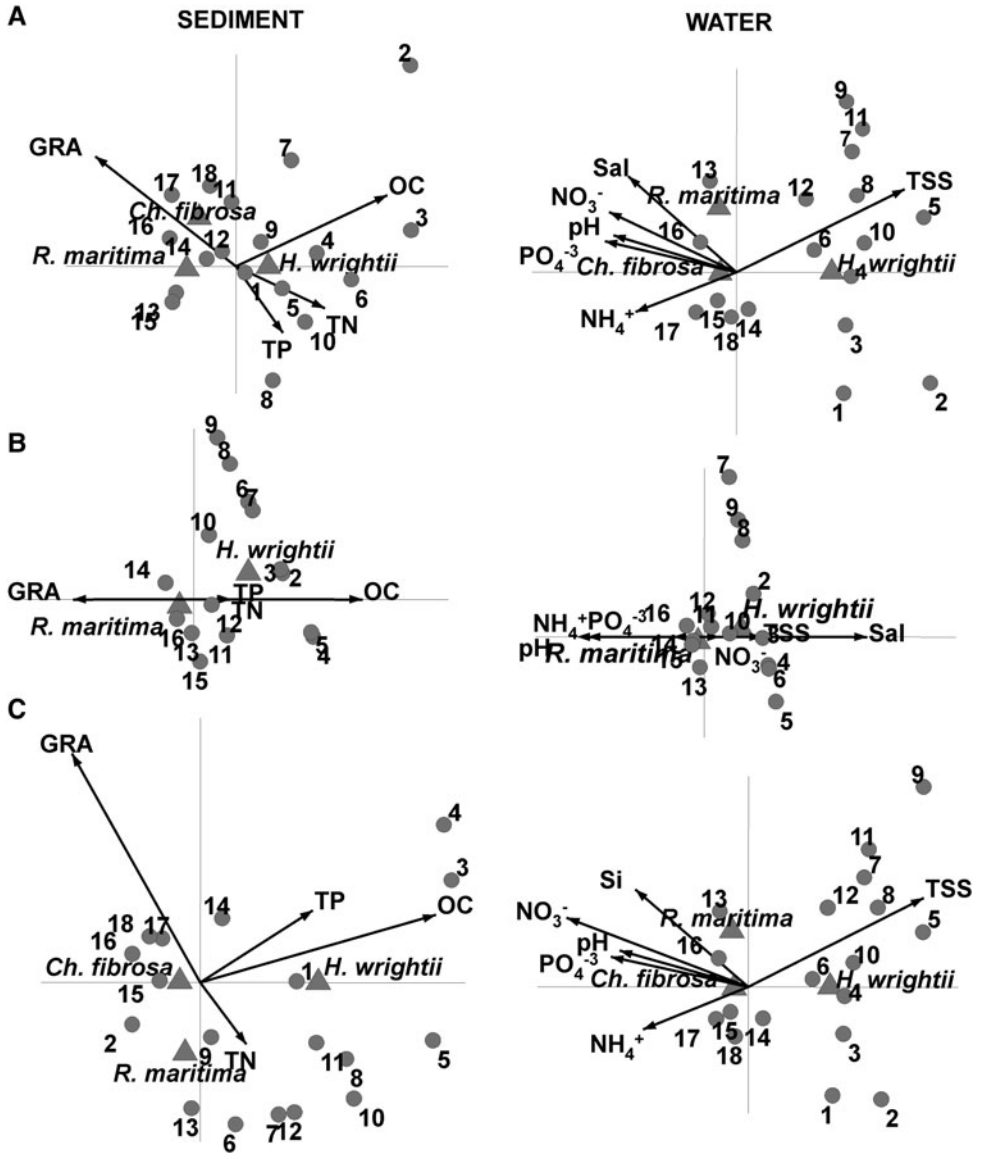

Fig. 5. Canonical correspondence analysis triplot variation in submerged aquatic vegetation (SAV) biomass and environmental variables in Celestun Lagoon in three climatic seasons: (A) Nortes, (B) Dry and (C) Rainy; SAV species (▲), environmental variables (arrows) and km (●). SAV species: *Halodule wrightii*, *Ruppia maritima* and *Chara fibrosa*. Variables estimated in the sediment: organic content (OC), total nitrates (TN), total phosphorous (TP) and grain size (GRA). Variables estimated in water: ammonium (NH_4^+), nitrates (NO_3^-), phosphates (PO_4^{-3}), salinity (Sal), silicates (Si), pH and total suspended solids (TSS).

gradient of the lagoon, whereas seasonal variations in biomass (total and discriminated by species) were best explained by OC, salinity and TSS. Concerning sediment variables, OC best explained spatial gradients in SAV biomass for Dry and Rainy seasons. This trend could be explained by a feedback process: SAV and microphytobenthos supply significant quantities of organic material (Kristensen *et al.*, 2008) and, at the same time, organic material (carbon) contributes to SAV production (Koch, 2001). OC showed highest concentrations between sites 3 and 9, where *H. wrightii* biomass was also highest, decreasing towards the inner zone of the lagoon.

Concerning water variables, ammonium in Nortes, salinity in the Dry season and TSS in the Rainy season mostly explained spatial variations in SAV biomass. Particularly, the strong salinity gradient along Celestun Lagoon was the most prominent feature of this ecosystem, exponentially decreasing from the mouth to the inner zone. A_o was greater in nitrate than in ammonium, reflecting a higher stability in the former. Average nitrate concentrations in the three climatic seasons were around the same value reported by Herrera-Silveira (2006) for this lagoon (10 μM) and others (<80 μM) (Soetaert & Middelburg, 2009; del Pozo *et al.*, 2010). In Yucatan, groundwater discharges are rich in nitrates (Herrera-Silveira, 1994), including Celestun Lagoon (Herrera-Silveira, 2006). Concerning ammonium, Herrera-Silveira (2006) obtained reference values of 8 μM in the lagoons of the Yucatán Coast, 12 μM in Celestun Lagoon, and the average for this kind of ecosystem is between 5 and 10 μM (Contreras *et al.*, 1996). Higher values obtained in the present study during Nortes (16.5 μM), Dry (23.4 μM) and Rainy seasons (13.3 μM) could be related to organic matter decomposition processes originated from the SAV and the mangrove forest that surrounds the lagoon (Zaldívar *et al.*, 2004). In addition, these values could indicate an increase in eutrophic conditions of the system, reflecting a deterioration

https://doi.org/10.1017/S0025315412000677 Published online by Cambridge University Press

of the habitat that could be mainly ascribed to an exponential increase through time in motor boat traffic and bottom trawl fishing, which fragments and unpins the SAV and increases the amount of decomposition material. In this context, seagrasses could disappear and even be displaced by e.g. seaweeds, particularly in cases with eutrophication, causing regime shifts where green meadows and clear waters are replaced with unstable sediments, turbid waters and hypoxia (Quammen & Onuf, 1993; Thomsen *et al.*, 2012). Increased deposition of fine-grain organic particles can also affect SAV growth either by increasing porewater nutrients or by producing phytotoxic reduced sulphur compounds (Kemp *et al.*, 2004 and references therein).

Marked seasonal differences in water variables (e.g. salinity in the Dry season and TSS in the Rainy season) could also determine differences in the amount of variance explained by multivariate techniques in relation to SAV abundance. Estuaries are highly susceptible to climate forcing (Kimmel *et al.*, 2009), and one of these effects is the annual timing and magnitude of freshwater flow via underground discharges: the scarce rainfall in the Dry season makes the habitat more saline. On the other hand, SAV can maintain clear water through the reduction of nutrients (Kemp *et al.*, 2004). In the Rainy season, TSS concentration became lower and at the same time SAV biomass was the highest of the three climatic seasons. In this way, within-year variations in climatic conditions drive ecosystem responses (Lehman, 2004).

In summary, the salinity gradient was the most important factor determining the spatial distribution of SAV along the estuarine lagoon. Other variables of importance were sediment OC and grain size, as well as water salinity and TSS. Their relative contribution varied seasonally. In this case, salinity could be considered as a key factor shaping patterns in occurrence, abundance and spatial structure of seagrass beds reinforcing the notion of seagrasses as sensitive species to spatio-temporal variations in estuarine conditions.

ACKNOWLEDGEMENTS

This work is part of the PhD thesis of A.M. Burgos-León at CINVESTAV Mérida. Financial support from Consejo Nacional de Ciencia y Tecnología (grant to A.M.Burgos-León) is acknowledged. We thank the Fishery and Chemical Laboratory staff for help during field and laboratory activities.

REFERENCES

Adams V.D. (1990) *Water and wastewater examination manual*. Michigan: Lewis Publisher Inc.

Arceo-Carranza D., Vega-Cendejas M.E., Montero-Muñoz J.L. and Hernández de Santillana M.J. (2010) Influencia del tipo de hábitat en las asociaciones nictimerales de peces en una laguna costera tropical. *Revista Mexicana de Biodiversidad. Universidad Nacional Autónoma de México* 81, 823–837.

Bach S.D., Thayer G.W. and LaCroix M.W. (1986) Export of detritus from eelgrass (*Zostera marina*) beds near Beaufort, North Carolina, USA. *Marine Ecology Progress Series* 28, 265–278.

Buchanan J.B. (1984) Sediment analysis. In Holme N.A. and Mcintyre A.D. (eds) *Methods for study of marine benthos*. London: Blackwell Scientific Publications, pp. 41–65.

Chávez E.A., Garduño M. and Arreguin-Sanchez F. (1993) Trophic dynamic structure of Celestun Lagoon, Southern Gulf of México. In Christensen V. and Pauly D. (eds) *Trophic models of aquatic ecosystems*. ICLARM Conference Proceedings 26, pp. 186–192.

Contreras E.F., Castañeda O., Torres R. and Gutiérrez F. (1996) Nutrientes en 39 lagunas costeras mexicanas. *Revista de Biología Tropical* 44, 421–429.

Cressie N. (1991) *Statistics for spatial data*. New York: John Wiley & Sons.

Cyrus D.P. and Blaber S.J.M. (1987) The influence of turbidity on juvenile marine fishes in estuaries. Part 1. Field studies at St Lucia on the southeastern coast of Africa. *Journal of Experimental Marine Biology and Ecology* 109, 53–70.

del Pozo R., Fernández-Aláez C. and Fernández-Aláez M. (2010) An assessment of macrophyte community metrics in the determination of the ecological condition and total phosphorus concentration of Mediterranean ponds. *Aquatic Botany* 92, 55–62.

Dent J.B. and Blackie M.J. (1979) *Systems simulation in agriculture*. London: Applied Science Publishers.

Dodkins I., Rippey B. and Hale P. (2005) An application of canonical correspondence analysis for developing ecological quality assessment metrics for river macrophytes. *Freshwater Biology* 50, 891–904.

Herrera-Silveira J.A. (1994) Spatial heterogeneity and seasonal patterns in a tropical coastal lagoon. *Journal of Coastal Research* 10, 738–746.

Herrera-Silveira J.A. (2006) Lagunas costeras de Yucatán (SE, México): investigación, diagnóstico y Manejo. *ECOTRÓPICOS Sociedad Venezolana de Ecología* 19, 94–108.

Istvánovics V., Honti M., Kóvacs A. and Osztoics A. (2008) Distribution of submerged macrophytes along environmental gradients in large, shallow Lake Balaton (Hungry). *Aquatic Botany* 88, 317–330.

Kemp W.M., Batuik R., Bartleson R., Bergstrom P., Carter V., Gallegos Ch.L., Hunley W., Karrh L., Korch E.W., Landwehr J.M., Moore K.A., Murray L., Naylor M., Rybicki N.B., Stevenson J.C. and Wilcox D.J. (2004) Habitat requirements for submerged aquatic vegetation in Chesapeake Bay: water quality, light regime, and physical–chemical factors. *Estuaries* 27, 363–377.

Kenworthy W.J., Wyllie-Echeverria S., Coles R.G., Pergent G. and Pergent-Martini Ch. (2006) Seagrass conservation biology: an interdisciplinary science for protection of the seagrass biome. In Larkum A.W.D., Orth R.J. and Duarte C.M. (eds) *Seagrass biology, ecology and conservation*. Dordrecht, The Netherlands: Springer, pp. 595–623.

Kimmel D.G., Miller W.D., Harding L.W. Jr, Houde E.D. and Roman M.R. (2009) Estuarine ecosystem response captured using a synoptic climatology. *Estuaries and Coasts* 32, 403–409.

Koch E.W. (2001) Beyond light: physical, geological, and geochemical parameters as possible submersed aquatic vegetation habitat requirements. *Estuaries* 24, 1–17.

Kristensen E., Bouillon S., Dittimar T. and Marchand C. (2008) Organic carbon dynamics in mangrove ecosystems: a review. *Aquatic Botany* 89, 201–219.

Larkum A.W.D., Orth R.J. and Duarte C.M. (eds) (2006) *Seagrasses: biology, ecology and conservation*. Dordrecht, The Netherlands: Springer.

Lazar A.C. and Dawes C. (1991) A seasonal study of the seagrass *Ruppia maritima* L. in Tampa Bay, Florida. Organic constituents and tolerances to salinity and temperature. *Botanica Marina* 34, 265–269.

Lehman P.W. (2004) The influence of climate on mechanistic pathways that affect lower food web production in Northern San Francisco Bay Estuary. *Estuaries* 27, 311–324.

Littler D.S. and Littler M.M. (2000) *Caribbean reef plants: an identification guide to the reef plants of the Caribbean, Bahamas, Florida, and Gulf of Mexico*. 2nd edition. Washington, DC: OffShore Graphics Inc.

Matheron G. (1963) Principles of geostatistics. *Economic Geology* 58, 1226–1266.

Matheron G. (1965) *La théorie des variables régionalisées et ses applications*. Paris: Masson et Cie, Éditeurs.

Orth R.J., Luckenbach M.L., Marion S.R., Moore K.A. and Wilcox D.J. (2006) Seagrass recovery in the Delmara Coastal Bays, USA. *Aquatic Botany* 84, 26–36.

Parsons T.R., Maita Y. and Lalli C.M. (1984) *A manual of chemical and biological methods for seawater analysis*. Oxford: Pergamon Press.

Pérez-Castañeda R. and Defeo O. (2004) Spatial distribution and structure along ecological gradients: peneid shrimps in a tropical estuarine habitat of Mexico. *Marine Ecology Progress Series* 273, 173–185.

Preen A.R., Lee Long W.J. and Coles R.G. (1995) Flood and cyclone related loss, and partial recovery, of more than 1000 km² of seagrass in Hervey Bay, Queensland, Australia. *Aquatic Botany* 52, 3–17.

Quammen M.L. and Onuf C.P. (1993) Laguna Madre: seagrass changes continue decades after salinity reduction. *Estuaries* 16, 302–310.

Raposa K.B. and Oviatt C.A. (2000) The influence of contiguous shoreline type, distance from shore, and vegetation biomass on nekton community structure in eelgrass beds. *Estuaries* 23, 46–65.

Ribeiro J., Bentes L., Coelho R., Gonçalves J.M.S., Lino P.G., Monteiro P. and Erzini K. (2006) Seasonal, tidal and diurnal changes in fish assemblages in the Ria Formosa lagoon (Portugal). *Estuarine, Coastal and Shelf Science* 67, 461–471.

Robertson G.P. (1987) Geostatistics in ecology: interpolating with known variance. *Ecology* 68, 744–748.

Robertson G.P. (2000) *GS + : geostatistics for the environmental sciences*. Plainwell, MI: Gamma Design Software.

Rossi R., Mulla D.J., Journel A.G. and Franz E.H. (1992) Geostatistical tools for modeling and interpreting ecological spatial dependence. *Ecological Monographs* 62, 277–314.

Short F.T. and McRoy C.P. (1984) Nitrogen uptake by leaves and roots of the seagrasses *Zostera marina* L. *Botanica Marina* 27, 547–555.

Short F.T., Carruthers T., Dennison W. and Waycott M. (2007) Global seagrass distribution and diversity: a bioregional model. *Journal of Experimental Marine Biology and Ecology* 350, 3–20.

Soetaert K. and Middelburg J.J. (2009) Modeling eutrophication and oligotrophication of shallow-water marine systems: the importance of sediments under stratified and well-mixed conditions. *Hydrobiologia* 629, 239–254.

Stirling H.P. (ed.) (1985) *Chemical and biological methods of water analysis for aquaculturalists*. Stirling, Scotland: Institute of Aquaculture, University of Stirling.

Strickland J.D.H. and Parsons T.R. (1972) *A practical handbook of seawater analysis*. Bulletin 167, Fisheries Research Bord of Canada.

Ter Braak C.J.F. (1986) Canonical correspondence analysis: a new eigenvector technique for multivariate direct gradient analysis. *Ecology* 67, 1167–1179.

Ter Braak C.J.F. and Smilauer P. (2002) *CANOCO reference manual and CanoDraw for Windows user guide: software for canonical community ordination (version 4.5)*. Ithaca, NY: Microcomputer Power.

Thomsen M.S., Wernberg T., Engelen A.H., Tuya F., Vanderklift M.A., Holmer M., McGlathery K.J., Arenas F., Kotta J. and Silliman B.R. (2012) A meta-analysis of seaweed impacts on seagrasses: generalities and knowledge gaps. *PLoS ONE* 7, e28595.

Touchette B.W. (2007) Seagrass–salinity interactions: physiological mechanisms used by submersed marine angiosperms for a life at sea. *Journal of Experimental Marine Biology and Ecology* 350, 194–215.

Travers M.J. and Potter I.C. (2002) Factors influencing the characteristics of fish assemblages in a large subtropical marine embayment. *Journal of Fish Biology* 61, 764–784.

Wagner H.H. (2003) Spatial covariance in plant communities: integrating ordination, geostatistics, and variance testing. *Ecology* 84, 1045–1057.

Zaldívar J.A., Herrera-Silveira J., Coronado-Molina C. and Parra D.A. (2004) Estructura y productividad de los manglares en la reserva de la biosfera Ría Celestún, Yucatán, México. *Madera y Bosques Número especial* 2, 25–35.

and

Zupo V., Mazella L., Buia M.C., Gambi M.C., Lorenti M., Scipione M.B. and Cancemi G. (2006) A small-scale analysis of the spatial structure of a *Posidonia oceanica* meadow off the Island of Ischia (Gulf of Naples, Italy): relationship with seafloor morphology. *Aquatic Botany* 84, 101–109.

Correspondence should be addressed to:
O. Defeo
UNDECIMAR, Facultad de Ciencias
Iguá 4225, Montevideo, Uruguay
email: odefeo@fcien.edu.uy

https://doi.org/10.1017/S0025315412000677 Published online by Cambridge University Press